



*Supplement of*

## **Temporal trends in methane emissions from a small eutrophic reservoir: the key role of a spring burst**

**Sarah Waldo et al.**

*Correspondence to:* Sarah Waldo (sarahrwaldo@gmail.com)

The copyright of individual parts of the supplement might differ from the article licence.

**Table S1: Measurement methods summary**

<i>Method</i>	<i>Flux Measured</i>	<i>Spatial Coverage</i>	<i>Frequency</i>	<i>Use</i>
Eddy Covariance (EC)	total net	~100s m <sup>2</sup> , north sector of the lake	pseudo-continuous, 30-min timestep	<ul style="list-style-type: none"><li>• annual budgets</li><li>• diurnal patterns</li><li>• biophysical drivers: ANN, Q10, 2DKS</li></ul>
Active Funnel Traps (AFT)	ebullition	0.3 m <sup>2</sup> , two locations	pseudo-continuous, 30-min timestep	<ul style="list-style-type: none"><li>• annual budgets</li><li>• diurnal patterns</li><li>• biophysical drivers: Q10, 2DKS</li></ul>
Flux Chamber	diffusion	0.2 m <sup>2</sup> per site	2 sites bi-weekly; 15 sites sampled during 6 GRTS surveys	<ul style="list-style-type: none"><li>• annual budgets</li><li>• emission pathway relative importance</li></ul>
Passive Funnel Traps	ebullition	0.3 m <sup>2</sup>	15 sites sampled during 6 GRTS surveys	<ul style="list-style-type: none"><li>• annual budgets</li><li>• spatial patterns</li><li>• emission pathway relative importance</li></ul>

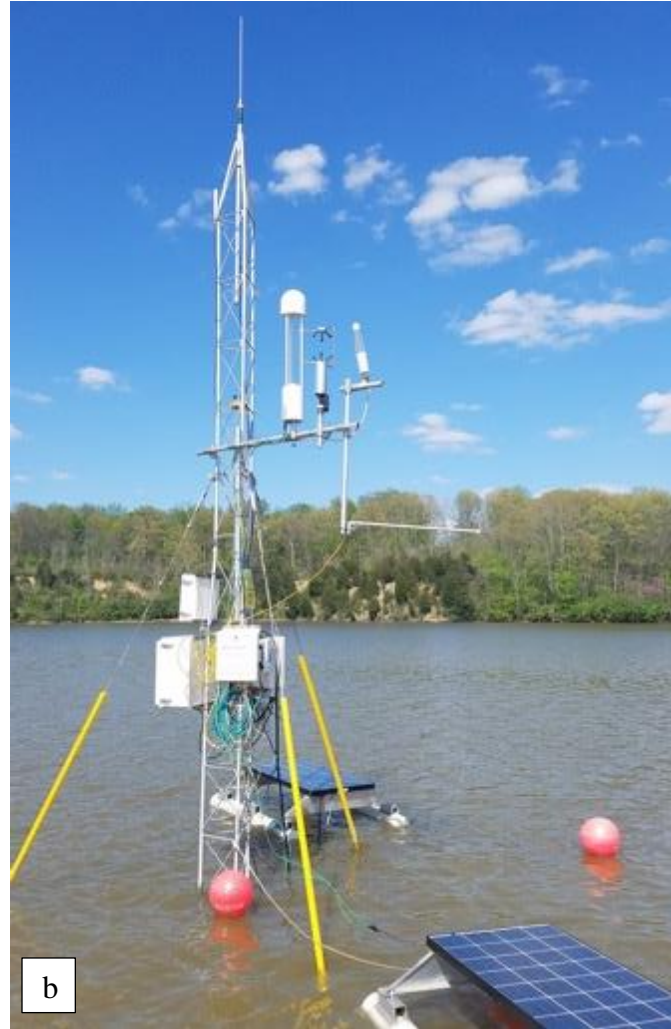


Figure S1: Pictures of eddy covariance measurement locations. Panel a (left): site S-1, dock location for February 2017 – April 2018 monitoring. Panel b (right): site S-2, open-water location for May – November 2018 monitoring.

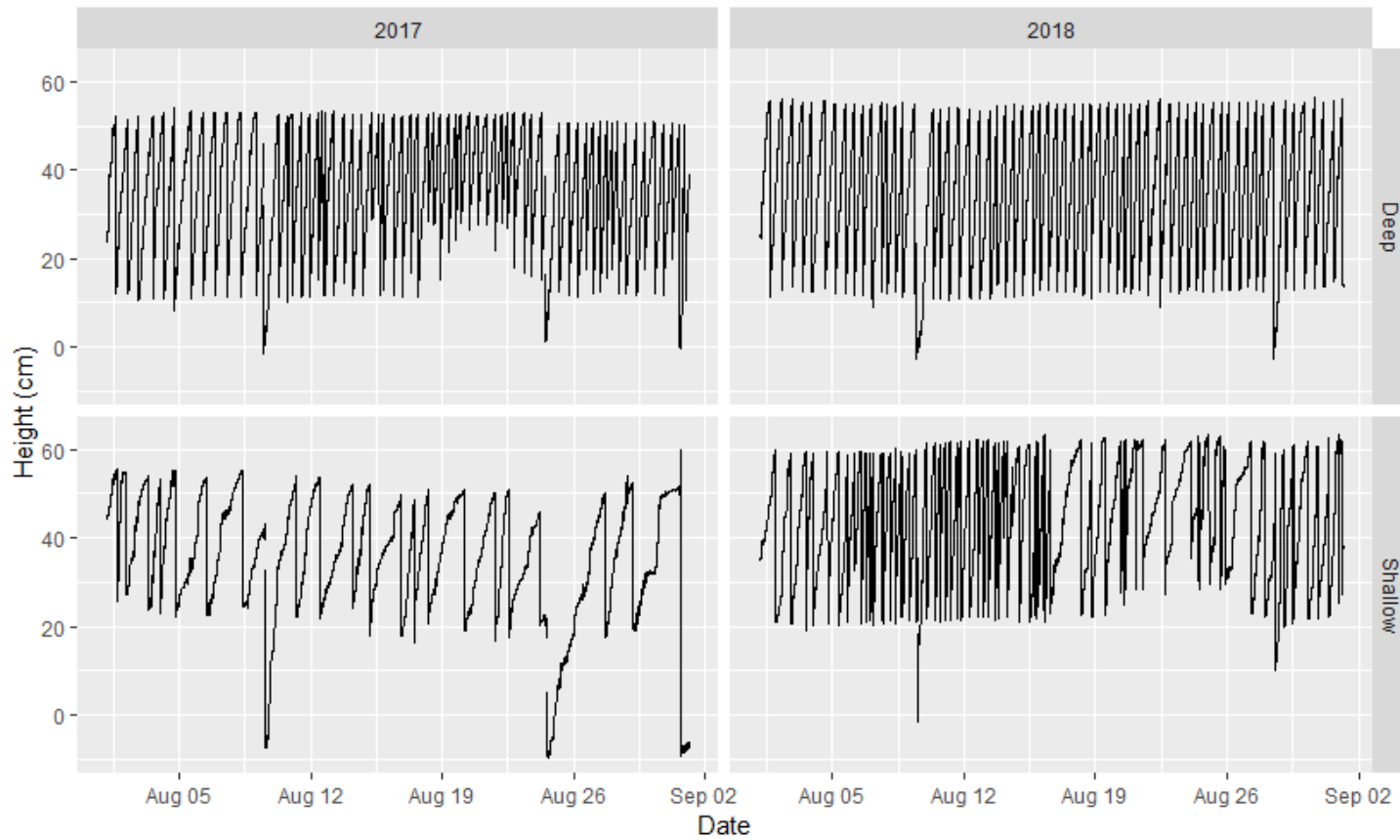


Figure S2: Time series of the raw active trap volume measurements from the two monitoring sites: the deep site (U-12, top), and the shallow site (U-14, bottom).

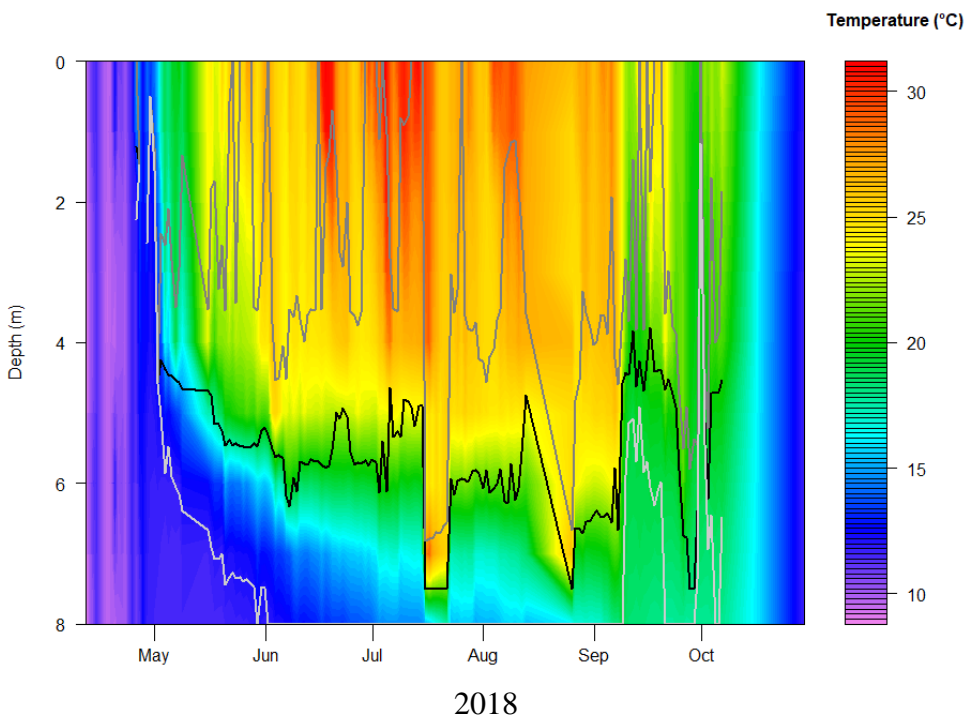
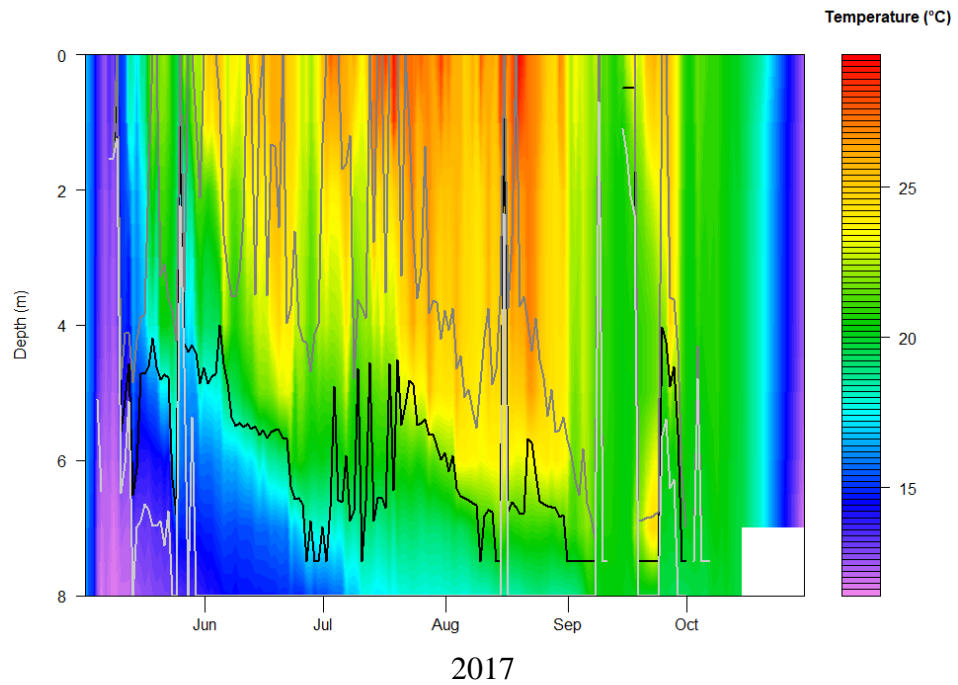


Figure S3: Time series of the water temperature profile including thermocline depth (black line) in 2017 (top) and 2018 (bottom) at the U-14 deep site in Acton Lake.

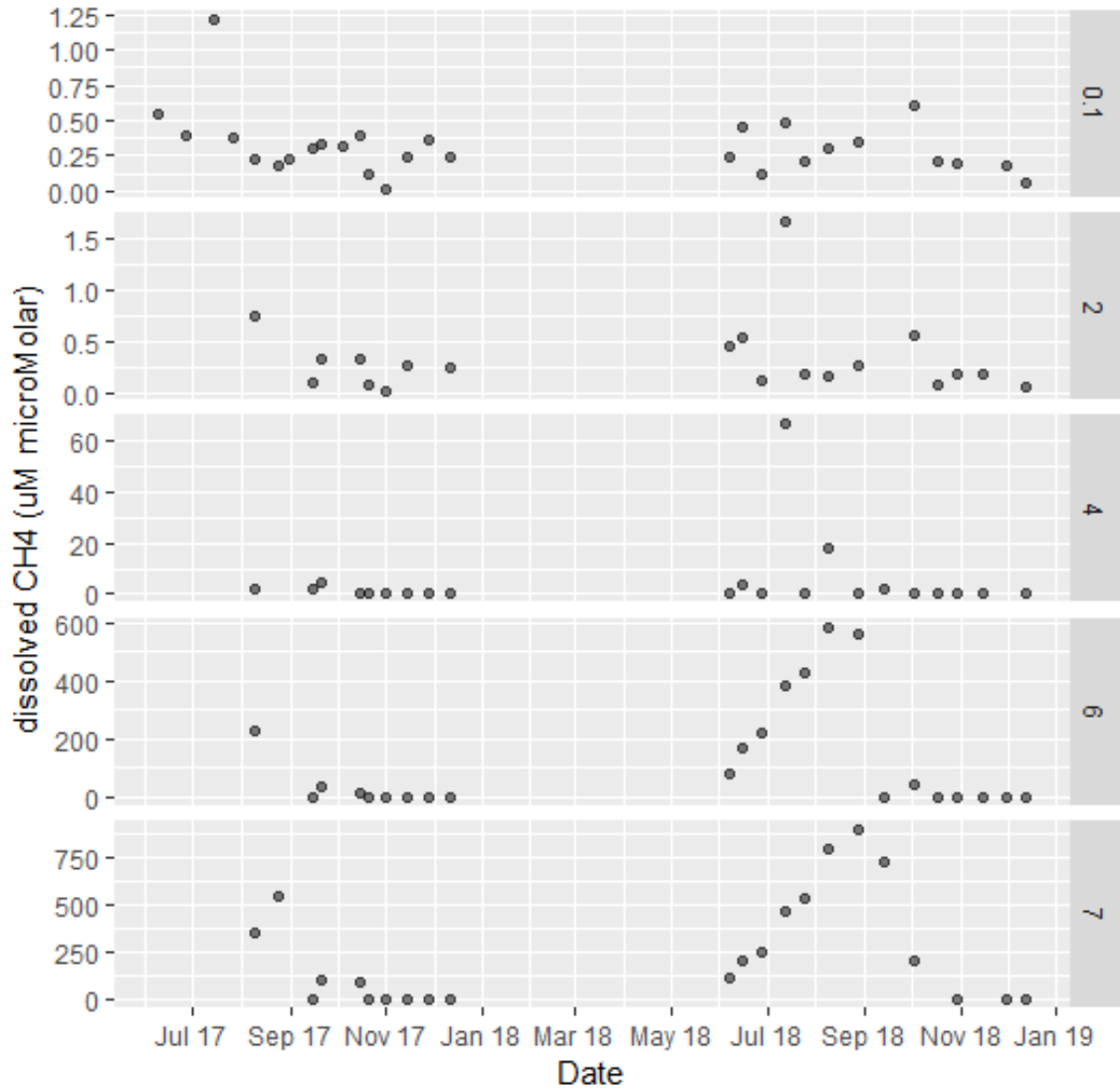


Figure S4: Time series of the depth profile of dissolved CH<sub>4</sub> (uM) at the deep site (U-14) over the 2017-2018 study period. Numbers on the right panels indicate depth in m below surface.

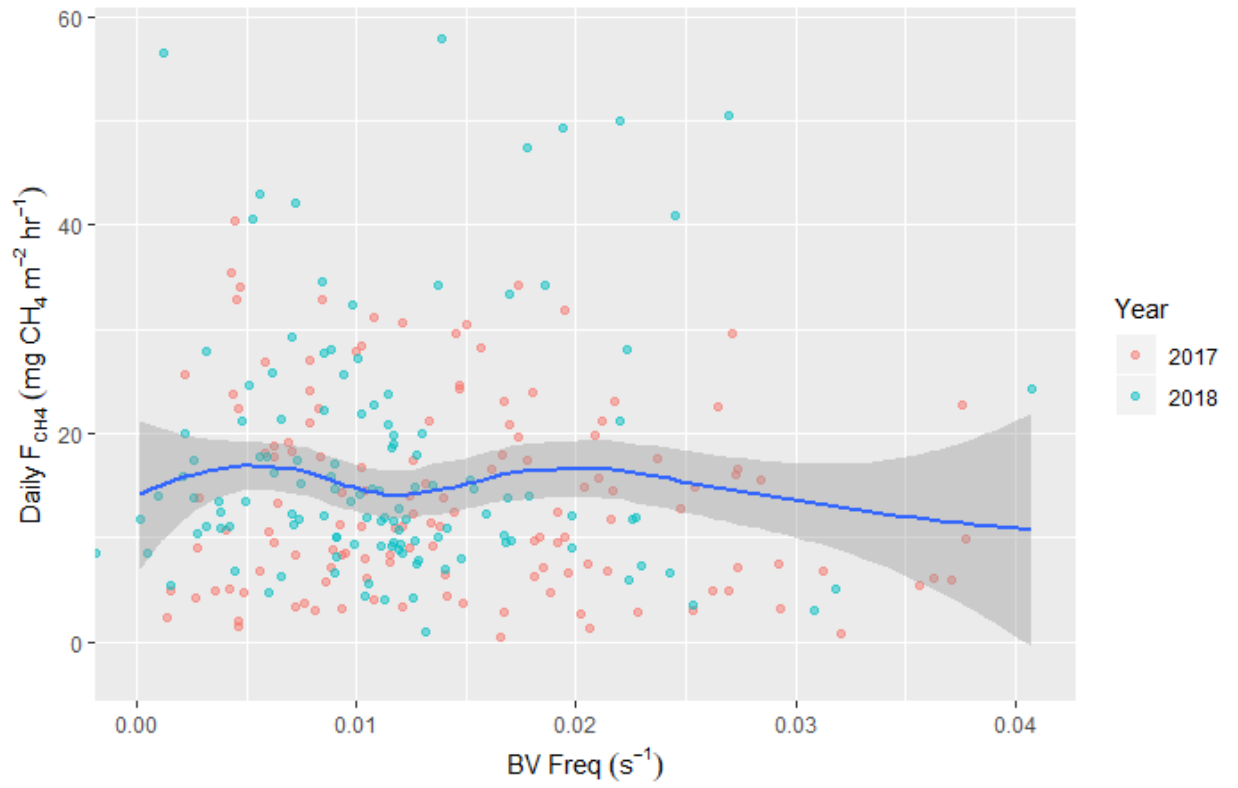


Figure S5: Scatterplot of daily  $F_{\text{CH}_4}$  as a function of the Brunt-Väisälä frequency, an indicator of underwater turbulence.



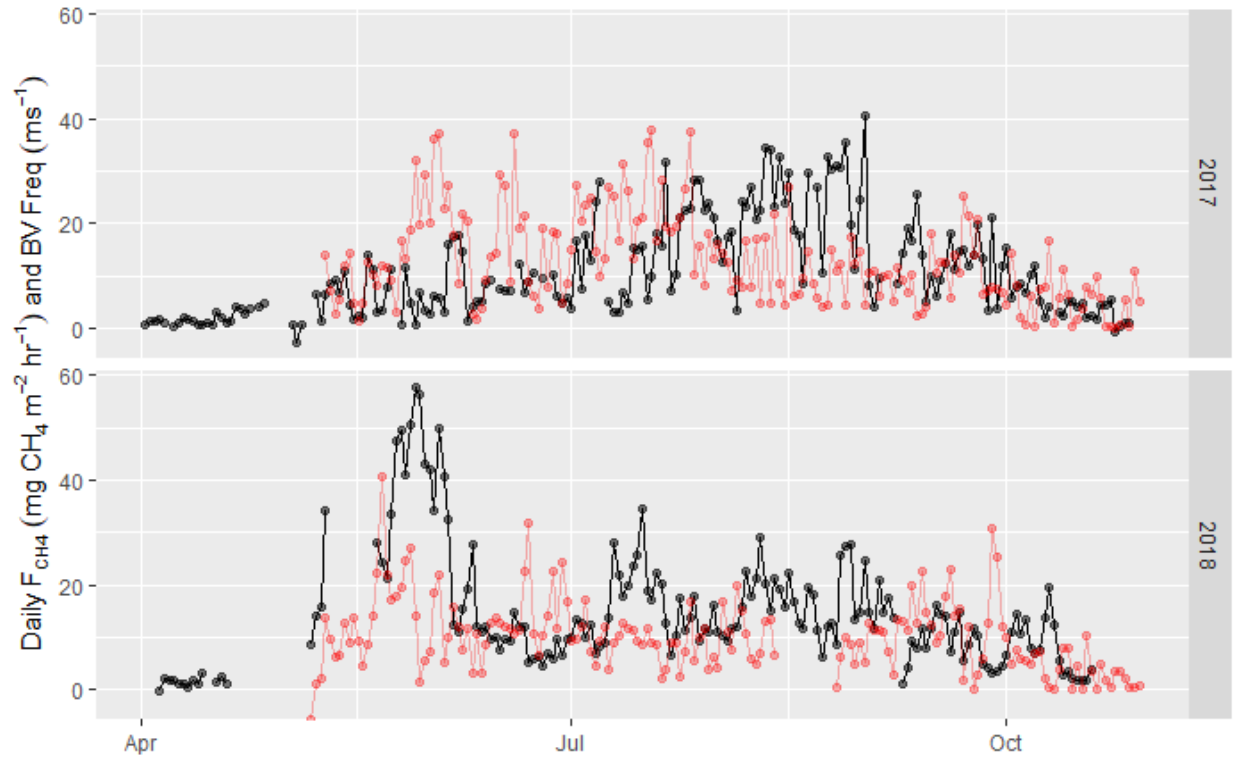
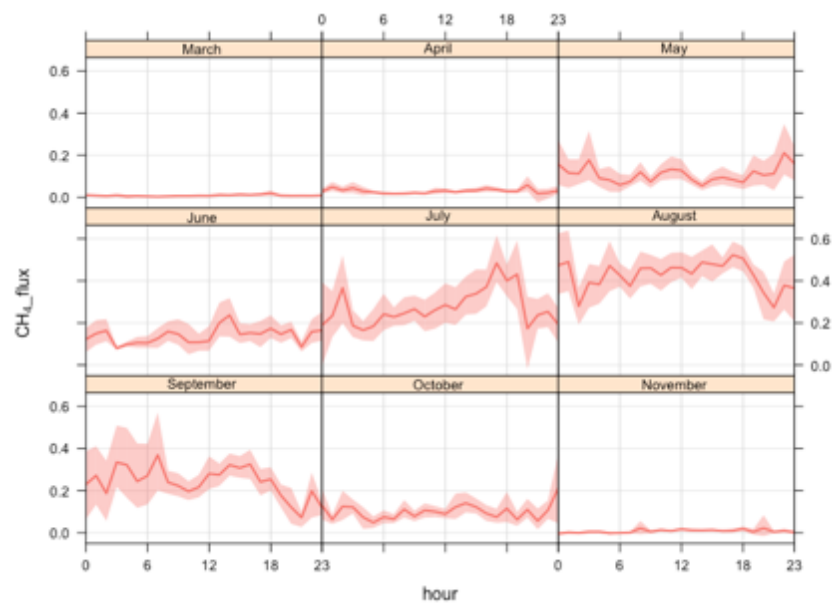
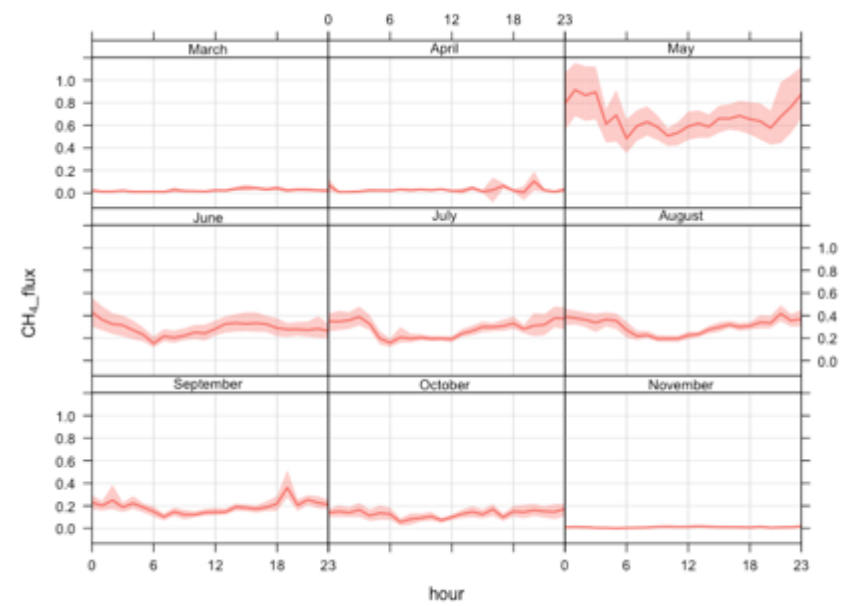


Figure S6: Time series of daily  $F_{\text{CH}_4}$  (black) and Brunt-Väisälä frequency (red) plotted on the same axes.



2017



2018

Figure S7: Diurnal  $F_{CH_4}$  ( $\mu\text{mol m}^{-2} \text{h}^{-1}$ ) aggregated over monthly time periods from March-Nov for 2017 (left) and 2018 (right).

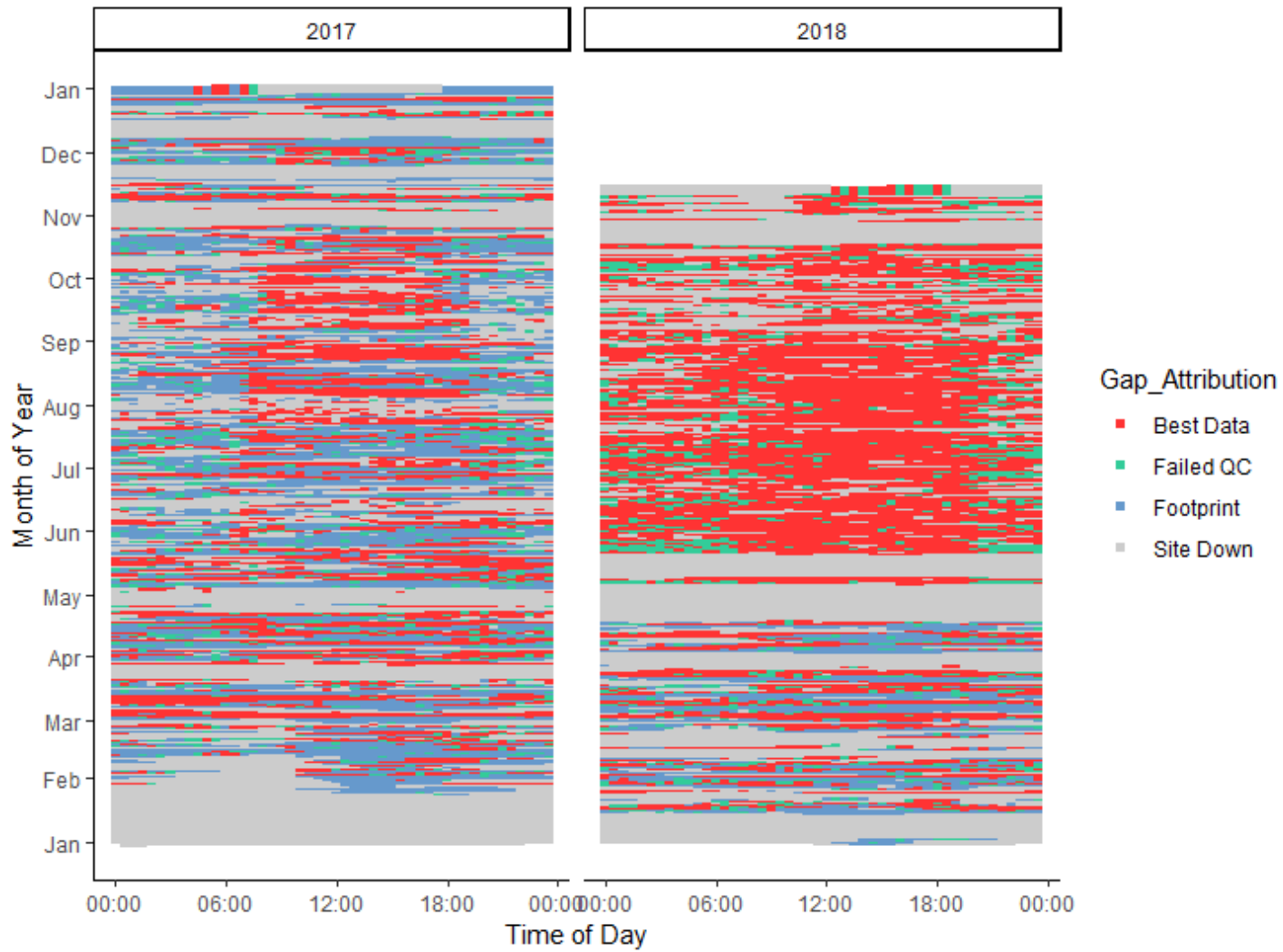


Figure S8: Eddy covariance gap attribution and distribution for 2017 and 2018. Each pixel represents one 30-minute flux measurement period.

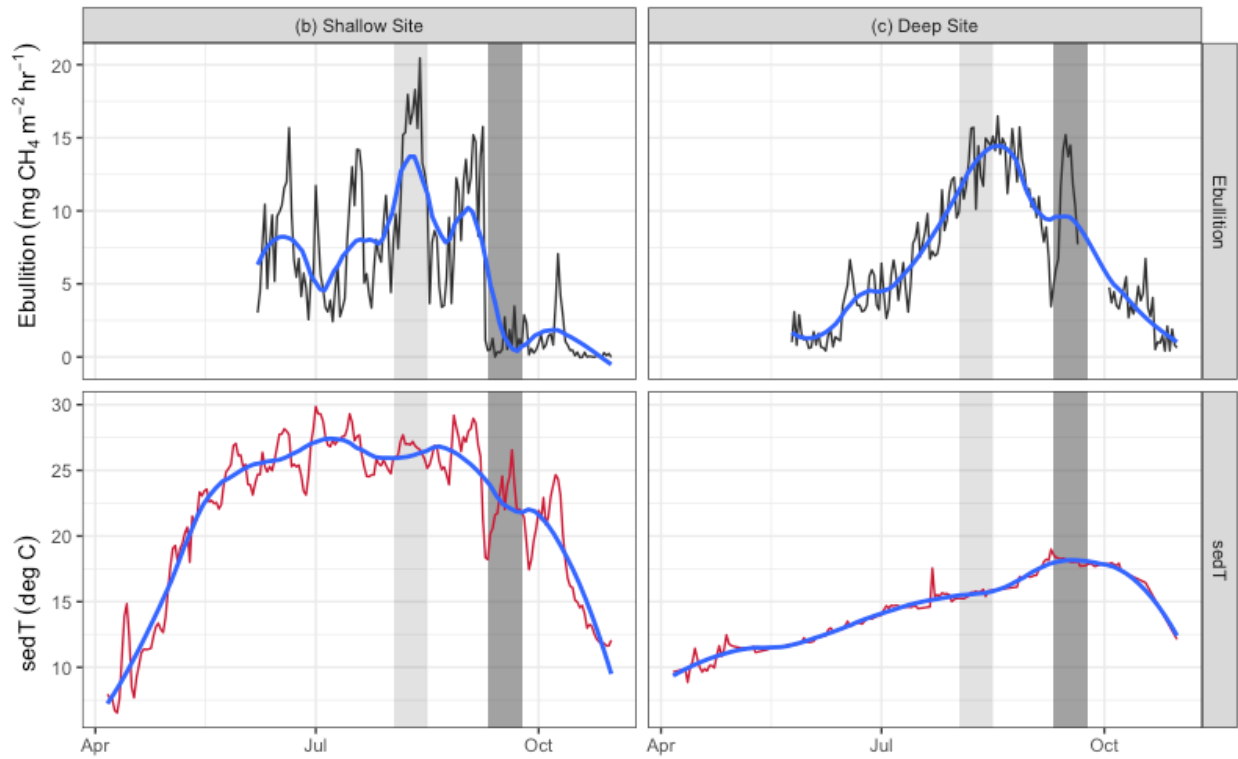


Figure S9: Time series of sedT and ebullition in 2018 at the shallow (a, U-14) and deep (b, U-12) sites. This year did not display the offset relationship between maximum sedT and maximum ebullition observed in 2017 (Fig. 10).

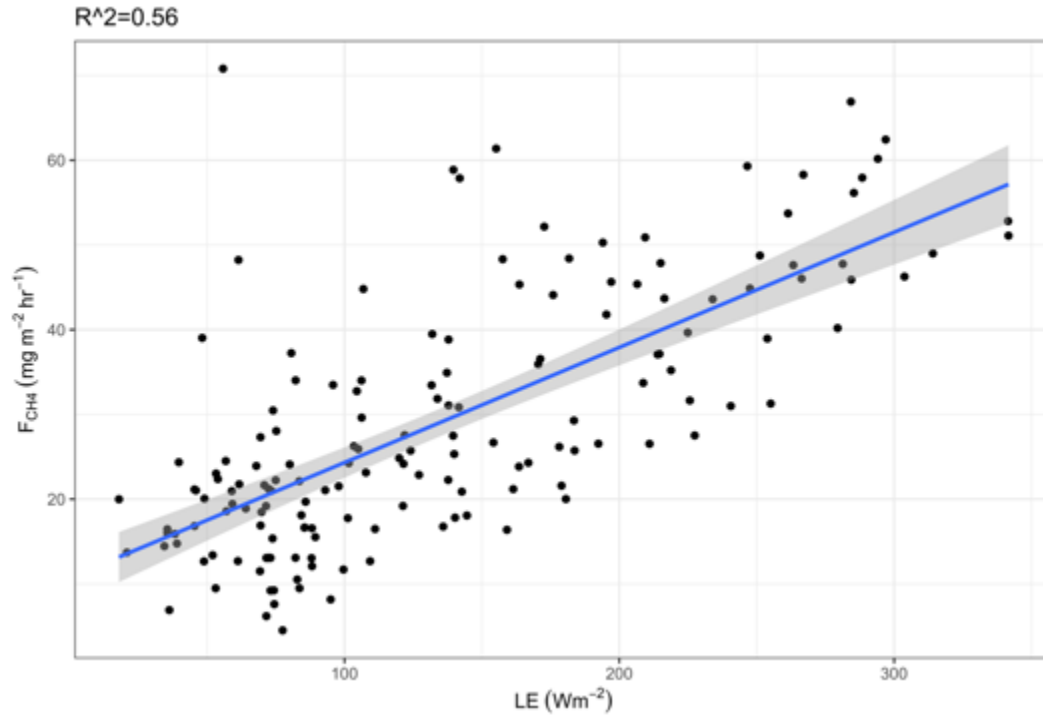


Figure S10: 30-minute methane fluxes as a function of latent heat flux (LE) for several-day period pre- and post-spring burst in 2018 (depicted in Fig 12 (a)). Significant at  $p<0.001$ .

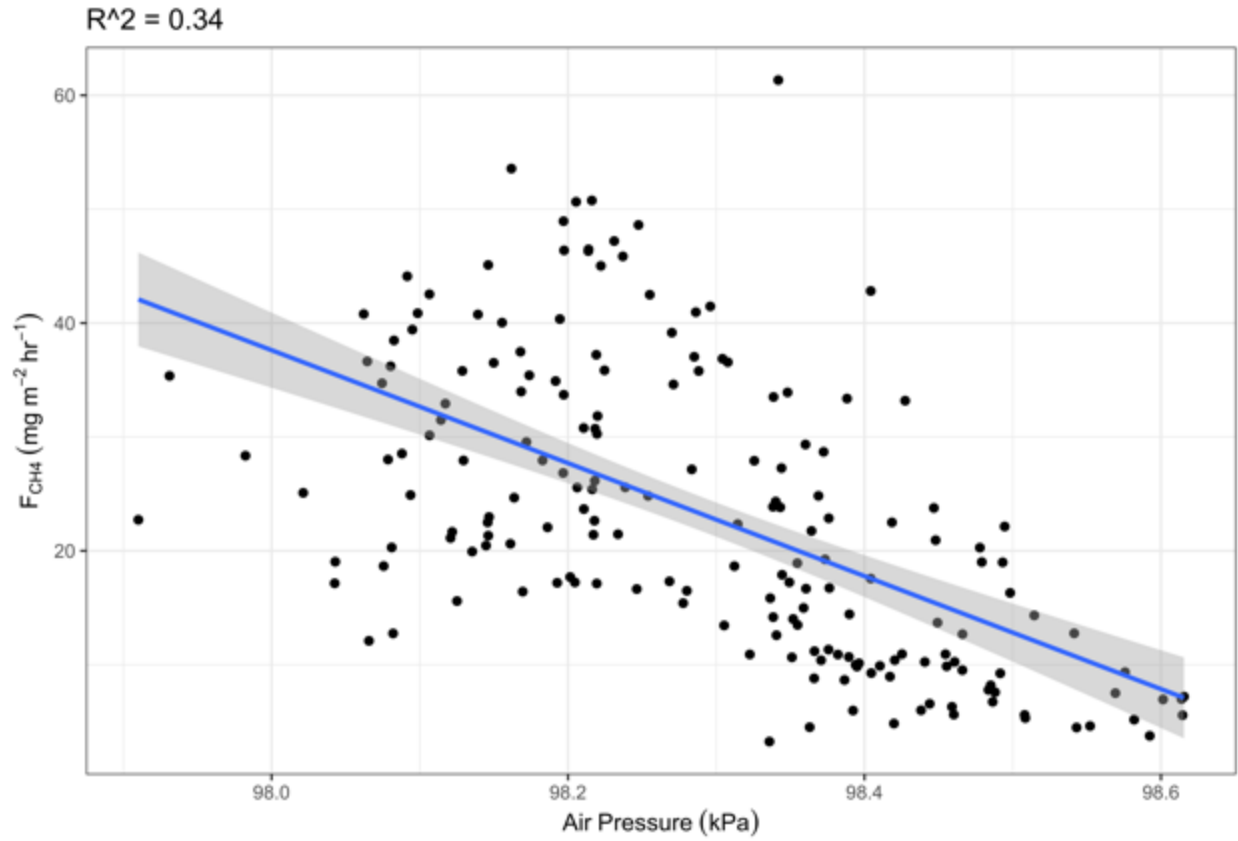


Figure S11: 30-minute methane flux as a function of air pressure for the several-day period depicted in Fig 12 (b). Significant at  $p < 0.001$ .